Effect of Tempering on the Toughness of a Cr-Mo Bainitic Steel

A.M. Nasreldin, M.M. Ghoneim, F.H. Hammad, R.L. Klueh, and R.K. Nanstad

The effect of tempering on impact and fracture toughness properties of a Cr-Mo bainitic steel was studied in the quenched and stress relieved (Q & SR) condition. The lowest tempering parameter used resulted in considerable improvement in impact properties. Further tempering increased the upper shelf energy, had a minor effect on the transition temperature, and increased both the initiation fracture toughness (J_{IC}) and the tearing modulus (T). However, the effect on J_{IC} and T was much greater than the effect on the impact upper shelf energy. The results were discussed in light of the changes in microstructure and flow properties due to tempering.

Keywords
bainitic steels, Cr-Mo steels, tempering, toughness

1. Introduction

THE microstructure/toughness relationship of bainitic steels has been the subject of considerable investigation in recent years. A limited amount of information is available concerning the effect of tempering on the impact properties of bainite microstructures. However, to our knowledge, no data have been reported on the variation of fracture toughness and tearing resistance with tempering for such a microstructure.

The complex microstructure of bainitic steels in the quenched and tempered condition is characterized by a highly dislocated lath structure arranged in packets, which subdivide the prior austenite grains. Carbide particles that precipitate during tempering are also present. These microstructural constituents are believed to control the level of toughness, because they would be expected to determine the propensity for cleavage and/or ductile fracture.

So far, there has been little agreement on the micromechanism that controls cleavage fracture in bainitic steels containing a lath microstructure. Some workers[1,2] have suggested that the packet size controls the fracture process, because high-angle packet boundaries can effectively impede the propagation of microcracks. Others[3,4] have shown that carbide size distribution is critical when cleavage is carbide induced. Conversely, a dislocation mechanism has been proposed[5] to explain the nondependence of cleavage fracture on either the carbide or the packet size.

In contrast to cleavage, the micromechanism of ductile fracture of quenched and tempered steels has been shown clearly[6] to proceed by the nucleation of voids around second-phase particles (inclusions and/or carbide particles) followed by the growth and coalescence of these voids. Both the dislocation density and second-phase shape, size, and distribution were found to be the effective microstructural parameters that govern the ductile fracture process.[6]

The nucleation of voids at second-phase particles occurs under the stress and strain fields ahead of a sharp crack or a round notch tip. The subsequent void growth and coalescence stages proceed by tensile-ductile rupture of the ligaments between the voids, or between the voids and the crack or notch tip. If the work-hardening capacity of the matrix is not sufficient for the ligaments to neck down, the growth stage is curtailed, and the ligaments fail by localized shear.[7]

In the present study, the effect of tempering treatment on the impact and fracture toughness parameters of a nonclassical form of bainite (produced by quenching) is investigated. The interrelation between the fracture behavior and the microstructural changes developed during tempering (i.e., dislocation density and carbide morphology and spacing, as evaluated through transmission electron microscopy) is discussed.

2. Experimental

Tests were performed on a commercial heat (A 9349) of a 3Cr-1.5Mo-0.1V steel developed at Climax Molybdenum Company.[8] The chemical composition is given in Table 1.

Table 1 Chemical composition of 3Cr-1.5Mo-0.1V steel

Element	Composition, wt%
C	0.12
Mn	0.84
Si	0.27
Ni	0.14
Cr	2.86
Mo	1.48
V	0.09
S	0.002
P	0.011
Al	0.004
Sn	0.002
Sb	<0.001
Cu	0.06
N	141 ppm

A.M. Nasreldin, M.M. Ghoneim, and **F.H. Hammad,** Atomic Energy Authority, Cairo, Egypt; and **R.L. Klueh** and **R.K. Nanstad,** Oak Ridge National Laboratory, Oak Ridge, Tennessee.

Table 2 Tensile properties of quenched and tempered 3Cr-1.5Mo-0.1V steel

Tempering parameter, *TP*	Yield strength (σ_y), MPa	Ultimate strength (σ_u), MPa	Elongation, % Uniform	Total	σ_y / σ_u
Q & SR(a)	1078	1261	5.3	17.4	0.85
19.6(b)	666	770	6.8	18.4	0.86
20.4(c)	497	626	8.5	22.3	0.79
21.0(d)	441	582	10.2	25.2	0.76

(a) Water quenched after 2 h at 955 °C and stress relieved for 2 h at 565 °C. (b) Q & SR + 8 h at 663 °C. (c) Q & SR + 16 h at 691 °C. (d) Q & SR + 30 h at 704 °C.

Table 3 Impact properties of quenched and tempered 3Cr-1.5Mo-0.1V steel

TP	TT-54J, °C	USE, J
Q & SR	67	136
19.6	−73	225
20.4	−70	232
21.0	−77	266

Tensile properties and details of the heat treatment are shown in Table 2.[8] The tempering parameter (*TP*) is defined as:

$$TP = Ta(20 + \log t)$$

where *Ta* is the absolute temperature in K, and *t* is time in h.

Charpy V-notch impact tests were conducted for the steel before and after the tempering treatment. Test temperature ranges were broad enough to determine upper shelf energy (USE) and ductile-to-brittle transition temperature (TT-54J). Fracture toughness tests were carried out at room temperature using 25.4-mm thick compact specimens. J-integral tearing resistance (J-R) behavior was determined using the single specimen unloading compliance (SSC) technique.[9] J-R curves produced from the SSC method were used to determine initiation fracture toughness (J_{IC}) and the tearing modulus (*T*).

Thin foils and carbide extraction replicas were examined by transmission electron microscopy (TEM). A detailed microstructural analysis is given elsewhere.[10]

3. Results

The impact properties of the 3Cr-1.5Mo-0.1V steel before and after the tempering treatment are given in Table 3. Note that the values of the transition temperature and USE for the quenched and stress relieved steel indicate poor toughness. Tempering of the steel to the lowest tempering parameter used, *TP* = 19.6, resulted in considerable improvement in the impact properties. TT-54J decreased by 140 °C, and USE increased by about 65%. As shown in Table 3 and Fig. 1, further tempering resulted in very little change in the transition temperature, whereas USE increased by about 18% between the lowest and the highest tempering parameters used.

Results of the J-integral tearing resistance tests are shown in Fig. 2. Typical J versus crack extension, Δa, plots (R curves) are shown. The variation of J_{IC} and *T* produced from the corresponding R curves for each tempering parameter is summarized in Table 4 and shown graphically in Fig. 3. Both J_{IC} and *T* increased with an increase in tempering parameter. Tempering caused *T* to increase by 244% compared to an 85% increase in J_{IC}.

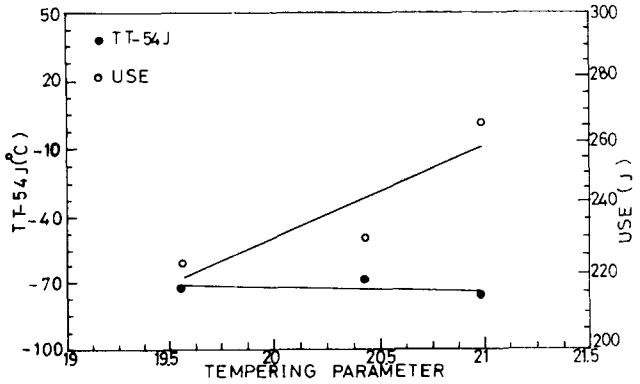

Fig. 1 Variation in transition temperature (TT-54J) and upper shelf energy (USE) of quenched and stress relieved 3Cr-1.5Mo-0.1V steel with tempering parameter.

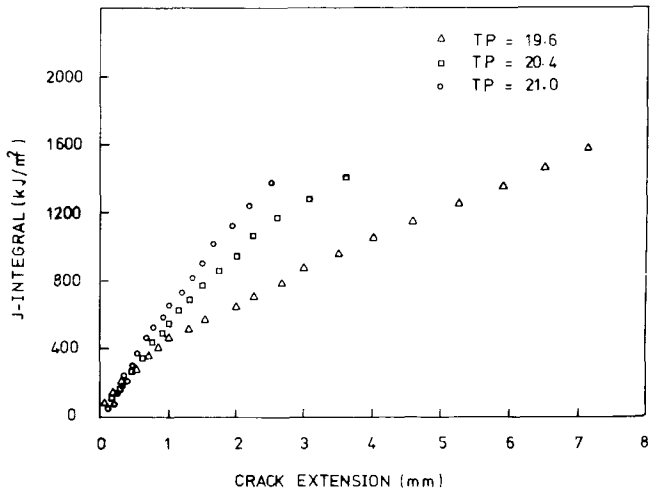

Fig. 2 J versus crack extension, Δa, of quenched and tempered 3Cr-1.5Mo-0.1V steel.

The quenched and tempered Charpy specimens, when tested at room temperature, exhibited completely ductile frac-

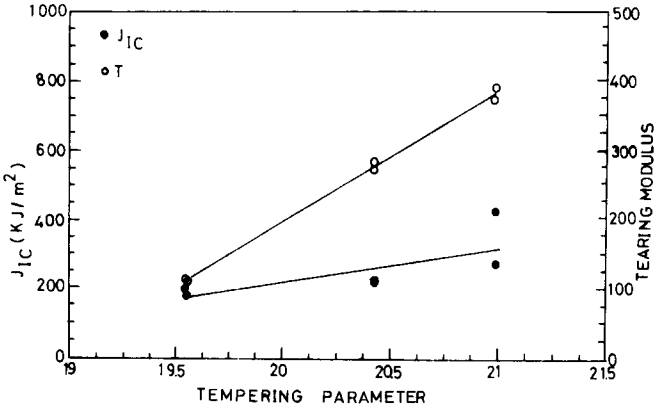

Fig. 3 Variation in initiation fracture toughness (J_{IC}) and tearing modulus (T) of quenched and stress relieved 3Cr-1.5Mo-0.1V steel with tempering parameter.

Table 4 Results of J-R tests of quenched and tempered 3Cr-1.5Mo-0.1V steel

TP	J_{IC}, kJ/m^2	*T*
19.6	176	110
	203	113
20.4	220	273
	217	285
21.0	275	375
	428	393

ture surfaces, indicative of upper shelf behavior. However, room-temperature tests of compact specimens of the same tempering conditions exhibited unstable (cleavage) fracture preceded by some stable ductile fracture. The fracture surfaces of these specimens are shown in Fig. 4. Such behavior has been observed before[11] and indicates that upper shelf behavior defined under conditions of dynamic loading, as with an impact Charpy test, cannot be relied on to preclude cleavage in fracture toughness specimens tested at the same temperature.

Another observation that warrants mention is the inverse relationship between the stable crack extension, Δa, and the tempering parameter. This is evident in the R curves shown in Fig. 2 and the photographs in Fig. 4, in which stable crack lengths of 6.9, 3.6, and 2.5 mm correspond to tempering parameters of 19.6, 20.4, and 21.0, respectively. In Fig. 2, very little change has occurred in the final J value (at which the specimen failed by cleavage) with an increase in the tempering parameter.

Optical metallography of the quenched and stress relieved steel revealed an acicular or lath microstructure that was grouped as packets within the prior austenite grains. The steel had an ASTM grain size of 8.[10]

Figure 5 shows the effect of tempering on the microstructure of foil specimens as revealed by TEM. The quenched and stress relieved steel had a carbide-free lath structure containing a high density of dislocations (Fig. 5a). Tempering resulted in a recovered microstructure; a large decrease in dislocation density occurred and a subgrain structure developed (Fig. 5b and c). After

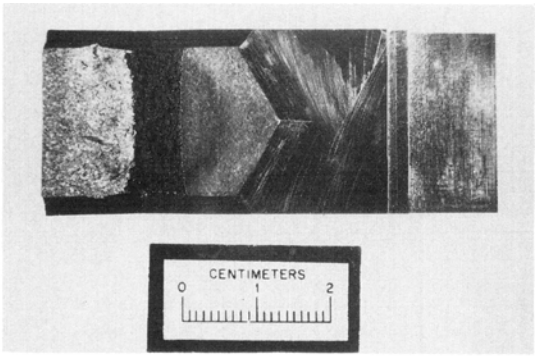

(a)

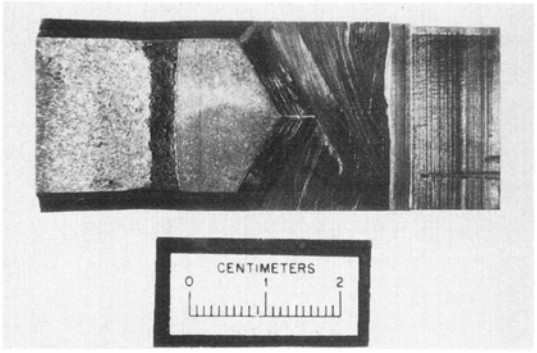

(b)

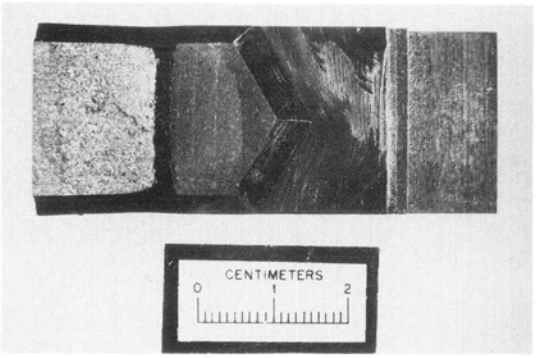

(c)

Fig. 4 Fracture surface of compact specimens at (a) *TP* = 19.6, (b) *TP* = 20.4, and (c) *TP* = 21.0.

tempering, precipitates were also observed within the matrix and on lath boundaries.

The carbide extraction replicas shown in Fig. 6 illustrate the effect of tempering on precipitate size, morphology, and spacing. At *TP* = 19.6, a mixture of precipitate sizes was observed (Fig. 6a). These included needlelike precipitates within the ma-

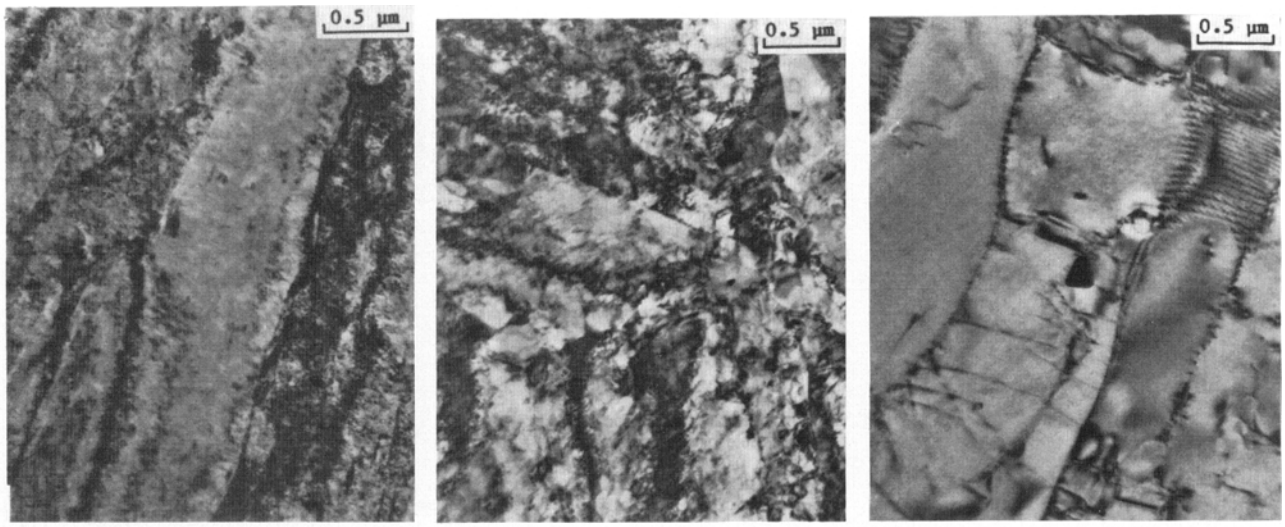

Fig. 5 TEM micrographs of 3Cr-1.5Mo-0.1V steel. (a) Quenched and stress relieved. (b) At $TP = 19.6$ and (c) at $TP = 21.0$.

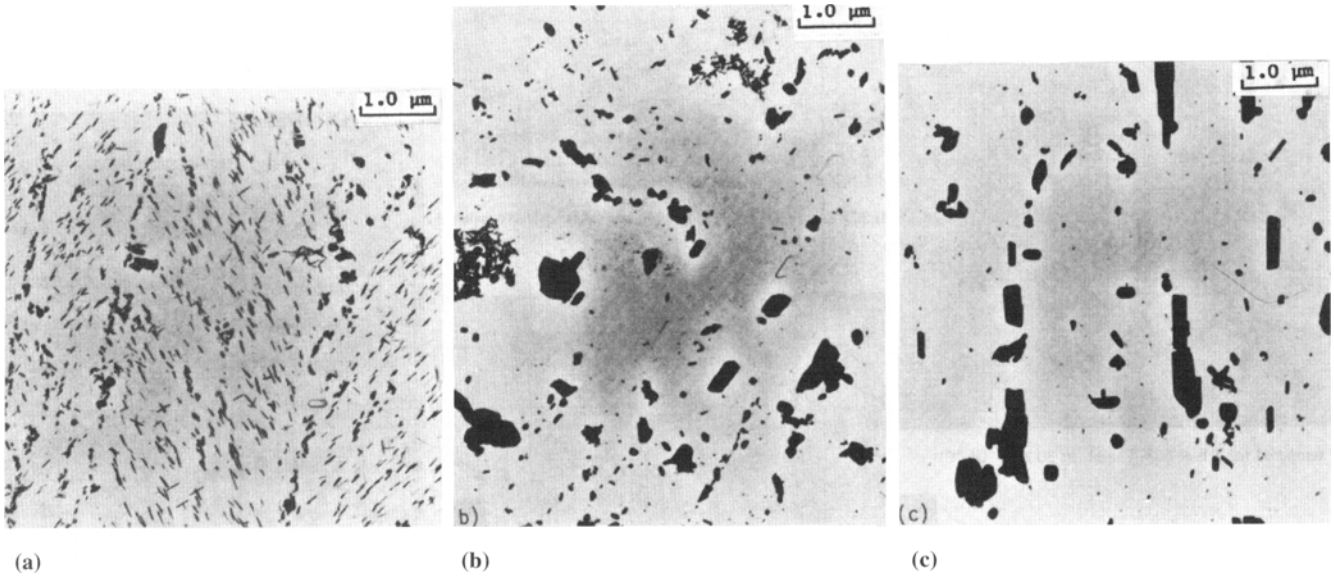

Fig. 6 Extraction replicas of 3Cr-1.5Mo-0.1V steel at (a) $TP = 19.6$, (b) $TP = 20.4$, and (c) $TP = 21.0$.

trix and along lath boundaries that were found to be mainly M_7C_3 carbides. After tempering to higher tempering parameters, these carbides coarsened, increased in spacing, changed into polygonal shape (Fig. 6b and c), and changed to $M_{23}C_6$ and M_6C carbide types.[10]

Although TEM replicas of the quenched and stress relieved steel did not reveal any kind of precipitates, carbide extraction results[10] indicated that some carbide precipitation occurred before tempering. Those results showed that the amount of carbides increased with increasing tempering parameter.

4. Discussion

The results have shown that before the tempering treatment (i.e., in the quenched and stress relieved condition) the steel exhibited poor impact properties, expressed by the fairly high transition temperature and the relatively low USE (Table 3). This can be associated with the high density of dislocations arising from the austenite-bainite transformation, as well as the residual internal stresses caused by the rapid rate of cooling

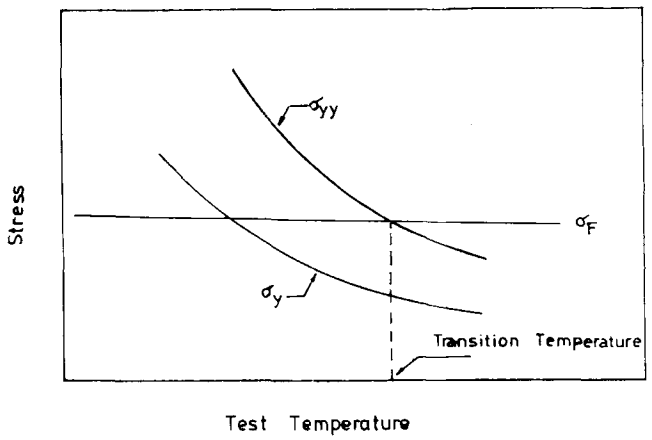

Fig. 7 Schematic showing the ductile-to-brittle transition temperature at the intersection of σ_{yy} and σ_F.

during quenching. These would enhance the nucleation of cleavage microcracks through a mechanism that may operate by piling up dislocations at carbide particles, leading to cracking of either the particle or the carbide/matrix interface.[7] As mentioned earlier, some carbide precipitation took place during the stress relief treatment, but the carbide size was too fine to be resolved by TEM. Therefore, cracking of the carbide/matrix interface would be more likely to occur and become the source of embrittlement.

In the test temperature range where ductile fracture occurs, the high density of dislocations in the matrix enhances the initiation of microvoids around the fine carbide particles present in the quenched and stress relieved steel. The low hardening capacity of the matrix could lead to a premature termination of the coalescence process of the expanding voids through rapid shear, which proceeds by localization of flow promoted by the high dislocation density.[12] The amount of energy consumed during the initiation and subsequent growth of voids is thus reduced appreciably. The result is that energy consumption through ductile fracture is limited both at the transition region and in the upper shelf range, thus increasing the transition temperature and reducing the USE value.

After tempering to the lowest tempering parameter used (*TP* = 19.6), impact properties improved considerably, as the transition temperature decreased by 140 °C and USE increased by 65% (Table 4). This improvement can be a direct consequence of the noticeable decrease in dislocation density due to recovery processes (Fig. 5b) and the extensive precipitation of carbide particles (Fig. 6a) during tempering. The precipitation of carbides would lead to a reduction of the solid solution strengthening elements (C, Mo, and Cr) in the matrix. This effect in addition to the decrease in dislocation density resulted in a substantially lower yield strength and an increase in the uniform elongation (Table 2). This indicates that an increase in the strain-hardening capacity occurs, although no decrease in σ_y/σ_u is observed. This would make it more difficult for the conditions for cleavage to be attained and would increase the tendency for the ductile mechanism of fracture. Therefore, microcracks, which may be induced at the needlelike carbide particles (Fig. 6a), will blunt out into voids instead of propagating in a brittle fashion, hence decreasing the transition temperature.

During the ductile fracture process, voids will nucleate at carbide/matrix interfaces under the influence of local dislocations tangled around carbide particles. Because the dislocation density has decreased markedly after tempering at *TP* = 19.6, it follows that additional deformation will be required to generate adequate dislocation density for the decohesion process. In addition, the improvement in strain-hardening capacity of the matrix will allow for an increase in the extent of void growth before coalescence takes place. The amount of energy expended during void initiation and growth processes is thus increased, leading to an increase in the upper shelf energy.

As shown earlier, tempering above *TP* = 19.6 (up to *TP* = 21.0) caused further microstructural changes. The dislocation density decreased (Fig. 5c) and the carbide particles increased both in size and spacing and changed into polygonal shapes (Fig. 6b and c). This was accompanied by a further reduction in yield strength, an increase in uniform elongation, and a decrease in σ_y/σ_u (Table 2), indicating a further increase in strain-hardening capacity. These changes in microstructure and flow properties should cause an improvement in the corresponding impact and fracture toughness parameters. The results showed such an improvement (Tables 3 and 4), except for the impact transition temperature, which was only slightly affected by the increase in tempering. This point is discussed below.

The increase in fracture toughness parameters J_{IC} and T with tempering can be caused by the same factors that influence USE, i.e., factors affecting void initiation and growth processes. However, the increase in J_{IC} due to additional tempering from *TP* of 19.6 to 21.0 was much higher than the corresponding increase in USE (85% versus 18%). This difference can be explained by the difference between stress and strain fields ahead of a sharp crack and a round notch. Stress and strain field gradients ahead of a sharp crack (as in a compact specimen) are steeper than those ahead of a round notch (as in a Charpy specimen).[13] Hence, the process zone, where void initiation and coalescence take place, is larger in the case of a round notch. Consequently, any change in carbide particle spacing with tempering would be expected to influence their chance to be located in the process zone of a sharp crack to a higher degree than in the case of a Charpy V-notch.

Table 4 shows that the increase in tearing modulus due to increasing tempering from *TP* of 19.6 to 21.0 was much higher than in J_{IC} (244% versus 85%). Other investigators have reported similar observations. Controlling the shape and volume fraction of inclusions in A516 grade 70 steel led to greater improvement in tearing modulus than in J_{IC}.[14] Also, it was found that degradation of tearing modulus due to neutron irradiation in A533-B steel was much higher than that for J_{IC}.[15] However, because the tearing modulus is defined as:[9]

$$T = (E/\sigma_f)dJ/da$$

where $\sigma_f = (\sigma_y + \sigma_u)/2$ and E is the elastic modulus, it can be expected that T will increase as σ_f decreases with tempering (Table 2). If this effect is excluded, the increase in dJ/da will be only 75%, which is comparable to the corresponding increase in J_{IC}.

As mentioned above, increasing the tempering parameter led to improvement of USE in impact testing and both J_{IC} and T in fracture toughness testing, but did not affect TT-54J in impact testing. By examining the fracture surface of impact specimens tested in the transition region, it was found that fracture starts in a ductile manner, and after some amount of stable ductile growth, cleavage occurred. Fracture behavior of compact specimens was quite similar, in that cleavage fracture was preceded by stable ductile crack extension (Fig. 4).

The process that causes a growing fibrous crack to change into the cleavage mode is in general not clear.[7] It is not even possible to judge safely whether cleavage is initiated directly from a stably growing ductile crack, or whether a ductile instability takes place first and then cleavage is triggered after a very small amount of rapid ductile fracture.[16] Physically, several explanations have been developed to account for ductile-initiated cleavage.[17] These assume that the local (tensile) stress, σ_{yy}, ahead of the propagating crack can be increased due to crack-tip sharpening, prestraining, and elevation of strain rate because of dynamic effects. Cleavage fracture is then expected to occur when this local stress exceeds the cleavage fracture strength, σ_F, of the material (Fig. 7).

Based on the above information, it can be argued that the factors that caused the observed nonvariation of the impact transition temperature with increasing tempering have produced that effect through their influence on σ_{yy} and/or σ_F. These factors are believed to be related to the changes in microstructure and flow properties due to increasing tempering. The local tensile stress, σ_{yy}, is a multiple of the material yield strength, σ_y. Thus, a decrease in σ_y will lead to a reduction in σ_{yy}. However, the multiplication factor (stress concentration factor), which is the value of the local tensile stress as normalized by the yield strength (σ_{yy}/σ_y), increases with an increase in strain-hardening capacity.[18] At the same time, an increase in the material strain-rate sensitivity is also expected to lead to an increase in σ_{yy}.

As shown above, the first tempering treatment ($TP = 19.6$) caused the yield strength to decrease from 1078 to 666 MPa. This was accompanied by a 22% increase in the uniform elongation, with no decrease in σ_y/σ_u (Table 2). This indicates a moderate increase in strain-hardening capacity. Comparatively, increasing tempering from $TP = 19.6$ to 21.0 decreased the yield strength from 666 to 441 MPa. The increase in strain-hardening capacity in this case was much higher, because the uniform elongation increased by 50% and σ_y/σ_u decreased from 0.85 to 0.78 (Table 2). Therefore, a larger decrease in σ_{yy} is expected to take place at $TP = 19.6$ than that after further tempering. Additionally, the ratio between the dynamic yield strength, as evaluated from instrumented impact testing, and the static yield strength was found to increase with increasing tempering,[19] indicating an increase in strain-rate sensitivity.

On the other hand, it was shown that the cleavage fracture strength, σ_F, of quenched and tempered structural steels is inversely proportional to the square root of the carbide size.[20] Accordingly, the observed increase in carbide size due to increasing tempering (Fig. 6) could have led to a reduction in σ_F for the present steel. Moreover, an element of material ahead of a growing crack is strained by the whole history of the process of growth up to the point when unstable fracture commences.[17] This prestrain process could reduce σ_F, the amount of reduction depending on the prestrain level. The prestrain level would be expected to increase as the material fracture toughness (J_{IC} and T) increases with tempering.

In light of the above discussion, the considerable decrease in the impact transition temperature, TT-54J, after the first tempering treatment ($TP = 19.6$) is related to the decrease in σ_{yy} associated with the large drop in the yield strength. The nonvariation in TT-54J on further tempering to $TP = 21.0$ can be attributed to the anticipated much smaller decrease in σ_{yy} in addition to the possible decrease in σ_F and the increased strain-rate sensitivity.

5. Conclusions

In this study, the effect of tempering treatment on the impact and fracture toughness of a 3Cr-1.5Mo-0.1V steel has been investigated. The following conclusions were reached. The lowest tempering treatment ($TP = 19.6$) produced significant improvement in both the impact transition temperature and the upper shelf energy. Further tempering (up to $TP = 21.0$) resulted in a smaller additional increase in upper shelf energy, but had very little effect on the transition temperature.

Increasing tempering from TP of 19.6 to 21 improved both the initiation fracture toughness, J_{IC}, and the tearing modulus, T. The increase in both parameters was higher than that in the upper shelf energy. The effect of tempering on impact and fracture toughness parameters is attributed to changes in microstructure and flow properties.

Acknowledgments

Thanks are due to members of the Metals and Ceramics Division, Oak Ridge National Laboratory (ORNL), for their technical assistance throughout this work. One of the authors (AMN) was on a fellowship at ORNL during the time the experimental part of this work was conducted.

References

1. P. Brozzo, G. Buzzichelli, A. Mascanzoni, and M. Mirabile, *Met. Sci.*, Vol 11, 1977, p 123-129
2. J.P. Naylor, *Metall. Trans. A*, Vol 10, 1979, p 861-873
3. D.A. Curry and J.F. Knott, *Met. Sci.*, Vol 12, 1978, p 511-514
4. P. Bowen and J.F. Knott, *Proc. 7th Int. Conf. on the Strength of Metals and Alloys*, ACSMA7, Vol 2, Pergamon Press, Oxford, 1985, p 1111-1115
5. D.A. Curry, *Met. Sci.*, Vol 18, 1984, p 67-76
6. J.F. Knott, *Proc. Int. Symp. Microstructure and Mechanical Behaviour of Materials*, IMMB, Xi'an, China, Vol 2, Chameleon Press, London, 1985, p 1073-1089
7. J.F. Knott, *Proc. 6th Int. Conf. Fracture*, ICF6, New Delhi, India, Pergamon Press, Oxford, 1984, p 83-103
8. R.L. Klueh and A.M. Nasreldin, ORNL-6206, Dec 1985
9. R.W. Swindeman, J.F. King, and R.K. Nanstad, ORNL/TM-9731, Sept 1985
10. R.L. Klueh and A.M. Nasreldin, *Metall. Trans. A*, Vol 18, 1987, p 1279-1290
11. F.J. Loss, NUREG/CR-0943, NRL Report-4064, 1979
12. J.F. Knott, *Met. Sci.*, Vol 14, 1980, p 327-336
13. T. Lin, A.G. Evans, and R.O. Ritchie, *Acta Metall.*, Vol 34, 1986, p 2205-2216

14. R.O. Ritchie and A.W. Thompson, *Metall. Trans. A*, Vol 16A, 1985, p 233-248

15. F.J. Loss, NUREG/CR-1128, NRL Report-4122, 1979

16. I.C. Howard and A.A. Willoughby, in *Developments in Fracture Mechanics*, Vol 2, G.G. Chell, Ed., Applied Science Publishers, London, 1983, p 39-99

17. E. Amar and A. Pineau, *Nucl. Eng. Design*, Vol 105, 1987, p 89-96

18. K. Wallin, T. Saario, and K. Torronen, *Met. Sci.*, Vol 18, 1984, p 13-16

19. A.M. Nasreldin, Ph.D. thesis, Cairo University, 1988

20. P. Bowen, S.G. Druce, and J.F. Knott, *Acta Metall.*, Vol 34, 1976, p 1121-1131